# Turkish Journal of Remote Sensing and GIS
## Türk Uzaktan Algılama ve CBS Dergisi

*Turk J Remote Sens GIS, September 2020, 1(2): 106-124*
*Journal homepage: http://www.dergipark.org.tr/en/pub/rsgis*

# Simulating Future Ecosystem Services of the Sokoto-Rima Basin as Influenced by Geo-Environmental Factors

## Jeo-Çevresel Faktörlerden Etkilenen Sokoto-Rima Havzasının Gelecekteki Ekosistem Servislerinin Simüle Edilmesi

**Saheed Adekunle Raji[1,2]*, Mayowa Fasona[2], Shakirudeen Odunuga[2]**

[1]*Federal University of Petroleum Resources, College of Science, Department of Env. Management and Toxicology Effurun/Nigeria.*
[2]*University of Lagos, Faculty of Social Sciences, Department of Geography, Akoka-Lagos/Nigeria.*

**ORIGINAL PAPER**

***Corresponding author:**
Saheed Adekunle Raji
raji.saheed@fupre.edu.ng

**doi:**

**Article history:**
Received: 11.07.2020
Accepted: 07.09.2020
Published: 30.09.2020

## Abstract

*Understanding the possible pattern of future ecosystem services can provide a systematic foundation for environmental resource management. This is vital towards science-based policy design, formulation, implementation, and review for the ecologically sensitive regions of the world such as the semi-arid West Africa. Therefore, the overarching objective of this study was to uncover the future ecosystem services of the Sokoto-Rima basin, particularly crop production (CP), seasonal water yield (SWY), habitat quality (HQ), and nutrient retention ratio (NRR) using InVEST software. Future (2050) land cover was constructed based on 2002, 2012 and 2015 Climate Change Initiative (CCI) remotely sensed data of the European Space Agency (ESA) using the artificial neural network algorithm of QGIS software. Results showed that CP averaged at 1.5 to 2.6 tons/km$^2$, indicating a low crop yield; annual SWY averaged at 464.64 mm, showing a low flow status; roughly 73% of the basin have low HQ; and NRR remains in the low category throughout the period of study. This suggests that scenario-based further assessment of ecosystem service interactions could be vital for sustainable land use policy.*

***Keywords***: *GIS, Semi-arid, Ecosystem services, Sokoto-Rima*

## Özet

*Gelecekteki ekosistem servislerinin olası modelini anlamak, çevresel kaynak yönetimi için sistematik bir temel sağlayabilir. Bu, yarı kurak Batı Afrika gibi dünyanın ekolojik olarak hassas bölgeleri için bilime dayalı politika tasarımı, formülasyonu, uygulanması ve gözden geçirilmesi için hayati önem taşımaktadır. Bu nedenle, bu çalışmanın genel amacı, InVEST yazılımını kullanarak Sokoto-Rima havzasının gelecekteki ekosistem servislerini, özellikle mahsul üretimi (MÜ), mevsimsel su verimi (MSV), habitat kalitesi (HK) ve besin tutma oranını (BTO) ortaya çıkarmaktır. Gelecekteki arazi örtüsü (2050), QGIS yazılımının yapay sinir ağı algoritması kullanılarak 2002, 2012 ve 2015 İklim Değişikliği Girişimi'nin (CCI) uzaktan algılanmış Avrupa Uzay Ajansı (ESA) verilerine dayanarak oluşturulmuştur. Sonuçlar, MÜ'nin ortalama 1,5 ila 2,6 ton/km$^2$ olduğunu ve düşük mahsul verimine işaret ettiğini, yıllık MSV ortalamasının 464,64 mm olduğunu ve bunun düşük akış durumunu gösterdiğini; havzanın yaklaşık %73'ünün düşük habitat kalitesine sahip olduğunu ve BTO'nun çalışma süresi boyunca düşük kategoride kaldığını göstermektedir. Bu durum, ekosistem servis etkileşimlerinin senaryoya dayalı olarak daha fazla değerlendirilmesinin, sürdürülebilir arazi kullanım politikası için hayati önem taşıyabileceğini göstermektedir.*

***Anahtar kelimeler***: *CBS, Yarı kurak, Ekosistem servisleri, Sokoto-Rima*

## 1. Introduction

Global attention on ecosystem services became intensified sequel to the publication of the Millennium Ecosystem Assessment (MEA) in 2005, which showed that roughly 70% of the 25 major ecosystem services of the Earth have either declined or are currently declining, thereby calling for a multi-scale and integrated approach towards reversing the trend (MEA, 2005a; MEA, 2005b; Setten et al. 2012; Wangai et al. 2016; Hølleland et al. 2017; Haines-Young & Potschin, 2018). The import of this call is borne out of the fact that vital human needs of food, shelter, water, medicine, climate regulation, pollution control and general wellbeing are directly and indirectly supplied by ecosystem services (MEA, 2005b). Therefore, natural supply of ecosystem services is directly proportional to socio-ecological and environmental dynamics. One key derivative from the MA report is the need to engage emerging scientific approaches in measuring, mapping and modeling ecosystem services dynamics towards sustainable use of ecological resources (Hølleland et al. 2017; Haines-Young and Potschin, 2018). The achievement of this goal however is a function of geography, sociocultural, economic and environmental value which is attached to the specific ecosystem service (Setten et al. 2012; Yang et al. 2018).

Given that the ability of an ecosystem to supply good and services is directly proportional to the functioning and integrity of that particular ecosystem, an altered environment such as dam construction for water, nutrient enhancement for soil fertility, and agricultural land expansion will proportionally impair the delivery of some ecosystem services (MEA, 2005b; Wangai et al. 2016; Haines-Young & Potschin, 2018). These activities could create rapid merits in terms of improved crop yield, increased water flow and enhance other consumption benefits in the short term; however, the long term consequences for biodiversity and other ecological losses could be severe. Natural responses to these dynamics is a function of ecological integrity and resilience of the particular ecological biome (MEA, 2005b; Roche & Campaigne 2017). Within semi-arid contexts, these scenarios have become normalized as land cover change (also referred to as land use change) remains the main driving force altering ecosystem services mostly driven by mono-directional policies such as agricultural improvement programmes, water supply enhancement schemes etc. (Yang et al. 2018). The manifestation of these events within a fragile ecosystem with brittle ecological balance presents a herculean challenge for environmental management (Yang et al. 2018; Wangai et al. 2016). It is therefore vital to spatially disentangle these ecosystem services and examine the nature and dynamics in the future for sustainable environmental management.

The Sokoto-Rima basin, a vital semi-arid ecological unit of northern Nigeria, is not immune to these realities. In this area, livelihood is tied to land where agriculture remains the lifeblood of the local economy. Despite this merit, natural dynamics of climate variability and change (Oguntunde et al. 2011), acute natural land degradation emanating from southward migration of the Sahara Desert (Oladipo, 1995; Olagunju, 2015), and multifaceted droughts of the 19th century (Oyebande and Odunuga, 2010) have altered the delivery of vital ecosystem services. These coupled with unsustainable agricultural practices such as overgrazing have led to ecosystem resource conflicts between crop farmers and migrant herdsmen (Fasona et al. 2007).

To guarantee the sustainability of the ecosystem services, management approaches that guarantee and synthesize status monitoring through mapping and future projections are vital (Huber et al. 2013). Such management approaches, driven by policy, will examine the dynamic factors that stimulate changes in the ecosystem services, track their transition pathways, and project future scenarios with respect to socioeconomic, ecological and environmental effects. Literature on the use the spatial tools of Remote Sensing and Geographic Information Systems (GIS) for simulating land cover and other geo-environmental factors for ecosystem services is on the rise. In a recent study, Satya et al. (2020) utilised GIS-based spatial factors to simulate future land use land cover scenarios of city of Warangal India and results showed that biophysical and socio-economic factors contributed to rise of built-up areas while agricultural land use will decline in the future. Fu et al. (2017) claimed that land use change influences variations in ecosystem services in mountainous areas of China. The study simulated units of provisioning ecosystem services to indicate heterogeneous nature of land use decisions on management of ecological resources. Yang et al. (2018) predicted that future ecosystem services are directly influenced by land use policy and climate in Yanhe watershed of northern Shaanxi Province of China.

The aim of this study was therefore to simulate the future ecosystem services of the Sokoto-Rima basin focusing on crop production, seasonal water yield, habitat quality and nutrient retention ratio. Specifically, the study was set to: (1) Examine the key geo-environmental factors that drive changes in land cover; (2) Quantify the current ecosystem services and; (3) model the future ecosystem services of the Sokoto-Rima basin using InVEST software package. This is with a view to examine the dynamics of changes in ecosystem services. The result of the study is expected to provide a suitable background for the assessment of ecological resources of the Sokoto-Rima basin.

## 2. Materials and Methods

### 2.1 The Study Area

Located in north-western end of Nigeria, Sokoto-Rima basin is a transnational catchment that extends beyond the boundary of Nigeria into neighboring countries, particularly Niger in the north and Benin Republic in the west. It is geographically confined to Latitudes 10˚32'35'' N to 13˚32'55''N and Longitudes 3˚30'30'' E to 8˚1'15''E with a total land area of 94,026.5 km$^2$ (see Figure 1). The ecosystem of the study area is greatly influenced by tropical savanna climate which is characterized by considerable seasonal variations. Annually, rainfall averages 350 mm in the north and 895 mm in the south while temperature is relatively high throughout the year, exceeding 30$^0$ C. Climate dynamics reflects on river flow characterization and ecosystem functioning with series of minor ephemeral streams that feed the major permanent rivers and lakes (Figure 1). Agriculture, particularly crop production and animal husbandry, is the lifeblood of the basin, hence, its settlement pattern is mainly rural. Crops such as rice, sorghum, millet, corn, beans, and groundnut are extensively cultivated on a small-scale and climate-reliant fashion.

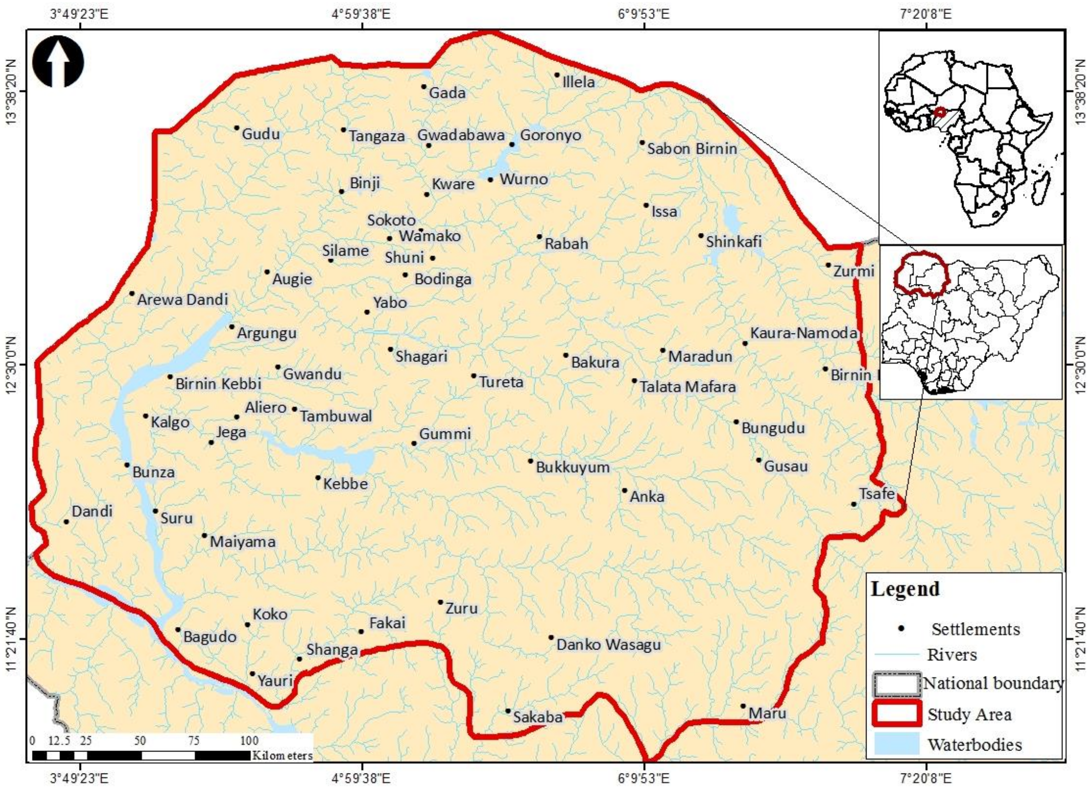


**Figure 1.** The study area in context of Africa and north-western part of Nigeria

### 2.2 Data Characteristics and Sources

The CCI (Climate Change Initiative) land cover data, a multi-sourced pre-classified remotely sensed data, was acquired from the portal of the European Space Agency (ESA). The data was processed from previously existing satellite data sources mainly: AVHRR (Advanced Very High Resolution Radiometer), Envisat MERIS (Medium Resolution Imaging Spectrometer), Sentinel-3 Ocean and Land Colour Instrument (OLCI), and Sea and Land Surface Temperature Radiometer (SLSTR). It has a spatial resolution of 300 meters and a dynamic range of 32 bits, which is suitable for an extensive basin such as the Sokoto-Rima. The pre-processed data was classified from source using a hybrid classification algorithm, which combines the strengths of supervised and unsupervised techniques (Defourny et al. 2016). It has 75% accuracy pre-tested during data validation task with GlobCover dataset (Defourny et al. 2016). Pérez-Hoyos et al. (2017) demonstrated the fitness of the data for cropland monitoring from continental to country level in Africa. However, data for the years 2002, 2012 and 2015 were acquired for the study.

Elevation, slope and aspect datasets were derived from ALOS World 3D Digital Surface Model (DSM) data acquired from the archives of JAXA (Japan Aerospace Exploration Agency). It has a horizontal resolution of one arc-second and 32-bit quantization depth. The eMODIS NDVI and evapotranspiration (ET) datasets were acquired from the USGS (United States Geological Survey) Famine Early Warning System (FEWS) data portal for West Africa. The datasets have a spatial resolution of 250 meters and a quantization level of 16 bits. Monthly rainfall and maximum temperature data covering climatic stations (Sokoto, Yelwa, Birnin Kebbi, Argungu, Gusau, Goronyo, Wurno, Kano, and Kaduna) within Nigeria were sourced from the Nigeria Meteorological Agency (NIMET) while supplementary climate data was sourced from Princeton University's station-based data from locations in Benin (Malanville) and Niger (Dabnou). The data spanned the years 1951 to 2015. Soil data (HYSOG Soil Group) was acquired from the portal of United States Oak Ridge National Library Distributed Active Archive Centre (ORNL DAAC). The data, which was developed in 2015, has a spatial resolution of 250 meters and 16-bit quantization level. Geology data was sourced from the defunct Federal Department of Agricultural Land Resources (FDAL) Kaduna Nigeria. It has a scale of 1:650,000. Population values and local government land areas were extracted from the archives of National Bureau of Statistics (NBS) 2010 version. These datasets were used to generate population density for each of the local government areas within the Sokoto-Rima basin.

## 2.3 Land cover Simulation

Simulation of the future land cover is based on the assumption that future land cover scenarios are governed by coupled human and natural systems (Lambin et al. 2003; Fasona et al. 2014). An algorithm that integrates top-down system dynamics with bottom-up cellular automata becomes the most apt due to its system coupling merits. MOLUSCE (Model for Land Use Change Evaluation), which is a spatially explicit QGIS plugin that permits the utilization of machine learning algorithm known as artificial neural network (ANN) with cellular automata (CA) to model future land cover patterns, was therefore adopted for the study. ANN facilitates the execution of fuzzy logic such that its algorithm works on multiple data structures and the output is binary-like. Its core element is designed to interact with connected neurons and the attached weight adjustment between the neurons. This process facilitates its ability to generate transition probabilities which is the chances of one data transforming into another based on the neuron connections within the multispectral data space. ANN thus permits the incorporation of series of geo-environmental variables as determinants of land cover change. The entire process was thus used to simulate 2015 and 2050 land cover data and validate with acquired land cover.

To set the model in MOLUSCE, land cover data of 2002 and 2012 alongside 13 geo-environmental variables (rainfall, temperature, elevation, slope, aspect, soil, geology, distance to road, distance to water body and distance to settlements, population density, and NDVI for 2002 and 2012) were set as input variables in the software. Pearson's correlation coefficient, which is a part of the MOLUSCE QGIS plugin, was used to check their level of multi-collinearity amongst these datasets.

## 2.4 Simulation Validation

Four model validation methods (Kappa for histogram information ($K_{hist}$), Kappa for pixel level location ($K_{loc}$) and overall kappa $K_{std}$ with percentage of correctness) as enunciated by Geri et al. (2011) were adopted. These are defined in equations (1), (2) and (3) as:

$$K_{hist} = \frac{P_{max} - P(Y)}{1 - P(Y)} \tag{1}$$

$$K_{loc} = \frac{P(X) - P(Y)}{P_{max} - P(Y)} \tag{2}$$

$$K_{std} = \frac{P(X) - P(Y)}{1 - P(Y)} \tag{3}$$

where: $P(X) = \sum_{i=1}^{c} p_{ij} = \sum_{i=1}^{c} p_{iT} p_{Tj}$ , $P_{max} = \sum_{1=i}^{c} \min(P_{iT} P_{Tj})$, $P_{ij}$ is the *i,j*th cell of the land cover contingency table, $P_{iT}$ is the total of all cells in the *i*th row, $P_{Tj}$ is the addition of all cells in the *j*th column, and *c* is the number of land cover categories.

## 2.5 Measuring Ecosystem Services

Sequel to the nature of the study area in terms of socioeconomics, dominant livelihood, biodiversity as well as data availability on ecosystem functioning, four ecosystem services were selected to be quantified, namely, crop production (CP), seasonal water yield (SWY), habitat quality (HQ), and nutrient retention ratio (NRR). Each of these were computed using the models enshrined in the InVEST (Integrated Valuation of Ecosystem Services and Trade-offs) and expressed as follows:

*Crop production*; The CP Regression Model was used for the study. It was based on separate computation of average yield of a given crop per land area within the multispectral space. Data requirements of the model include land cover, and crop fertilization rates identified with agricultural land use with inherent local climate. Mathematically, the model was defined by Mueller et al. (2012) as stated in equation (4):

$$Y_{modGC} = min\,(Y_{max}(1 - b_{NP}\,exp\,(-c_N N_{GC})), Y_{max}\,(1 - b_{NP}\,exp\,(-c_P P_{GC})), Y_{max}\,(1 - b_K\,exp\,(-c_K K_{GC}))) \quad (4)$$

where: $Y_{modGC}$ is yield for a particular crop (tonnes/km$^2$); $Y_{max}$ is maximum yield; $b_{NP}$ and $b_K$ are the y-intercepts for each nutrient-yield response curve; $c_N$, $c_P$, and $c_K$ are response coefficients that describe the percentage of $Y_{max}$ attained at a given nutrient level; $N_{GC}$ $P_{GC}$ $K_{GC}$ are the crop-based fertilization rates for rice, sorghum, millet and groundnut stated in Table 1. Modeled yield for each crop was added using raster math in ArcGIS 10.5 to produce the overall CP value (tonnes/km$^2$).

**Table 1**. Specific crop fertilization rates used for CP model (Tarfa et al. 2017)

| S/N | Crop name | Nitrogen rate | Phosphorous rate | Potassium rate |
|---|---|---|---|---|
| 1 | Rice | 100.0449 | 22.03867 | 33.0196 |
| 2 | Sorghum | 64.0113 | 14.0059 | 25.2265 |
| 3 | Millet | 60.3244 | 13.0096 | 12.1201 |
| 4 | Groundnut | 58.0119 | 22.1017 | 35.0112 |

*Seasonal water yield*; The SWY Model was used to quantify water yield in the Sokoto-Rima basin. It calculates the average amount of available water within a parcel of land as a function of the land cover and represents the quickflow of the basin. The Sokoto-Rima basin has a tropical continental climate where water availability is restricted to the wet season which spans June to August, an evidence of clear seasonality. Data required by the model includes monthly evapotranspiration, monthly rainfall, land cover, basin outlay, and digital elevation model (DEM). The SWY model is mathematically described in equations (5) and (6):

$$QF_{i,m} = n_m * \left( \left(a_{i,m} - S_i\right) exp\left(-\frac{0.2S_i}{a_{i,m}}\right) + \frac{S_i^2}{a_{i,m}} exp\left(\frac{0.8S_i}{a_{i,m}}\right) E_1\left(\frac{S_i}{a_{i,m}}\right)\right) * (25.4 \left[\frac{mm}{in}\right] \quad (5)$$

where: $S_i = \frac{100}{CN_i} - 10\ [in]$, $CN_I$ is the curve number for pixel *i*, a function of the local land cover and soil type; $a_{i,m}$ is the mean rain depth on a rainy day at pixel *i* on month *m*, and $E_1$ is the exponential integral function, $E_1(t) = \int_1^\infty \frac{e^{-t}}{t} dt$ in which *t* is the time study period.

The yearly quickflow which is the aggregate of the monthly (*m*) is given as:

$$QF_i = \sum_{m=1}^{12} QF_{i,m} \quad (6)$$

*Habitat quality*; The Habitat Quality model stated in InVEST was used to quantify HQ. The model hypothesizes that spatial patterns of biodiversity can be estimated using land cover distribution with respect to localized spatial threats. This approach was adopted as a measure of ecosystem biodiversity and its capacity to estimate spatial habitat degradation across the study area. Based on the level of socio-economic development of the study area, cultivated lands, settlements, railways lines, main roads and proximity to waterbody were identified as spatial threats and thus integrated to the model. Sharp et al. (2018) described the HQ model, which is mathematically expressed as:

$$Q_{xj} = H_j\left(1 - \left(\frac{D_{xj}^z}{D_{xj}^z + k^z}\right)\right) \quad (7)$$

where $Q_{xj}$ is habitat quality of cell *x* in land cover *j*, $D_{xj}^{z}$ is associated total threat level within the multispectral space *x* and *j*, *z* (hard coded =2.5) and *k* (half-saturation constant was set as 0.5) are scaling parameters.

*Nutrient retention ratio*; The Nutrient Delivery Ratio Model was used to quantify NRR. The model hypothesizes a nutrient cycling mass balance approach, which explains the spatial movement of nutrients under the influence of vegetation, rainfall and crop utilization of nutrients. DEM, land cover, nutrient load parameter, retention efficiency and length and nutrient runoff proxy (rainfall) were the datasets required by the model. The derived equation for NRR is given as:

$$NRR = 1 - \frac{NRE}{NT} \tag{8}$$

where: *NRR* (nutrient retention ratio) is the fraction of nutrients retained at a pixel position. *NT* (nutrient transport) is a measure of nutrient flow across from a pixel position to another. NRR ranges between 0 and 1 indicating no and maximum retention ratio, respectively.

## 3. Result and Discussion

### 3.1 Multicollinearity Test Analysis of the Geo-environmental Variables

The test for multicollinearity as revealed by Pearson's correlation measured at $\alpha$= 0.05 level of significance is presented in Table 2. Although the returned correlation coefficient showed direct (positive) and indirect (negative) linear association correlation, no degree of multicollinearity was detected. Overall, the relationship between the geo-environmental variables that could trigger or indicate the presence of multiple collinearity linkages was low (the computed *r* was less than 0.7). This shows that causally irrelevant variables have been eliminated and the variables are therefore suitable for future land cover simulation.

**Table 2.** Pearson's Correlation matrix of the geo-environmental variables

| | Aspect | NDVI (2012) | Rain | Pop den | Elev. | Temp. | Soil | Dist. to set | NDVI (2002) | Geol | Dist. to road | Slope | Dist. to water |
|---|---|---|---|---|---|---|---|---|---|---|---|---|---|
| **Aspect** | - | 0.02 | 0.02 | -0.01 | 0.01 | -0.02 | 0.02 | 0.02 | 0.02 | 0.01 | 0.02 | 0.22 | -0.01 |
| **NDVI (2012)** | | - | 0.07 | -0.12 | 0.16 | -0.19 | 0.02 | 0.12 | 0.48 | 0.03 | 0.13 | 0.02 | -0.02 |
| **Rainfall** | | | - | -0.27 | -0.14 | -0.16 | 0.11 | 0.13 | 0.25 | 0.20 | -0.06 | 0.08 | -0.04 |
| **Pop. den.** | | | | - | -0.15 | 0.24 | -0.04 | -0.16 | -0.19 | -0.05 | -0.06 | -0.02 | 0.10 |
| **Elev.** | | | | | - | -0.61 | -0.13 | 0.06 | 0.30 | 0.17 | 0.13 | 0.15 | -0.25 |
| **Temp.** | | | | | | - | -0.01 | -0.11 | -0.36 | -0.25 | -0.14 | -0.06 | -0.07 |
| **Soil** | | | | | | | - | -0.06 | 0.05 | 0.14 | -0.07 | -0.07 | -0.11 |
| **Dist. to set** | | | | | | | | - | 0.24 | -0.19 | 0.36 | 0.01 | 0.01 |
| **NDVI (2002)** | | | | | | | | | - | 0.14 | 0.19 | 0.07 | -0.09 |
| **Geol** | | | | | | | | | | - | -0.09 | 0.05 | -0.08 |
| **Dist. to road** | | | | | | | | | | | - | 0.02 | 0.04 |
| **Slope** | | | | | | | | | | | | - | -0.02 |
| **Dist. to water** | | | | | | | | | | | | | - |

### 3.2 Spatiotemporal Dynamics of Land cover

Since the functioning of ecosystems and the capacity to provide goods and services are analogous to dynamics on land, it is essential to scrutinize the nexus between the various natural and anthropogenic activities on land as indicated the dynamics of land cover characterization. Details of spatiotemporal change in the mapped land cover classes for the Sokoto-Rima basin are presented in Table 3 for the period 2002 to 2012.

As an agrarian landscape, cropland dominated the land cover in 2002 with land area of 68,470.94 $km^2$ which is almost three-quarters of the land proportion at 72.82%. Other land cover themes include agroforestry (11,843.30 $km^2$), shrubland (1,838.41 $km^2$), grassland (8,487.87 $km^2$), waterbody (3,043.92 $km^2$), settlement (81.90 $km^2$), bare surface (73.53 $km^2$), and woodland (186.64 $km^2$) occupying 12.6%, 1.96%, 9.02%, 3.24%, 0.09%, 0.08% and 0.20% of the land area, respectively. A decade after, in 2012, the land cover proportions returned similar distributions compared to 2002 with minuscule differences in some land cover themes. Specifically, cropland, waterbody, settlement, bare surface and woodland increased to 68,797.03 $km^2$ (73.17%), 3,056.43 $km^2$, (3.25%), 147.62 $km^2$, (0.16%), 90.55 $km^2$, (0.10%), 187.02 $km^2$, (0.20%) respectively. Agroforestry, shrubland and grassland reduced to 11,808.13 $km^2$ (12.56%), 1,692.01 $km^2$ (1.80%), and (8,247.72 $km^2$, 8.77%), correspondingly.

Pattern of change indicated that that cropland, waterbody, settlement, bare surface and woodland increased spatiotemporally by 0.35% (326.08 $km^2$), 0.01% (12.51 $km^2$), 0.07% (65.73 $km^2$), 0.02% (17.019 $km^2$), and 0.0004% (0.38 $km^2$), respectively (Table 3). Equally, agroforestry, shrubland and grassland contracted by -0.04% (-35.17 $km^2$), -0.16% (-146.4 $km^2$) and -0.26% (-240.14 $km^2$), respectively. It can be summed that land cover losses in the Sokoto-Rima basin is mainly dominated by natural landscapes which were replaced by anthropogenic activities particularly crop cultivation. The observed trend is anticipated to have consequences on the provisioning and regulating ecosystem goods and services which remain the prime source of sustenance in the Sokoto-Rima basin.

**Table 3**. Land cover change statistics for the Sokoto-Rima basin from 2002 to 2012

| Land cover classes | Land cover (2002) ($km^2$) | Land cover (2012) ($km^2$) | Change in land area ($Km^2$) | 2002 (%) | 2012 (%) | Proportion of change (%) |
|---|---|---|---|---|---|---|
| **Cropland** | 68,470.94 | 68,797.03 | 326.08 | 72.82 | 73.17 | 0.35 |
| **Agroforestry** | 11,843.30 | 11,808.13 | -35.17 | 12.60 | 12.56 | -0.04 |
| **Shrubland** | 1,838.41 | 1,692.01 | -146.40 | 1.96 | 1.80 | -0.16 |
| **Grassland** | 8,487.87 | 8,247.72 | -240.144 | 9.03 | 8.77 | -0.26 |
| **Waterbody** | 3,043.92 | 3,056.43 | 12.51 | 3.24 | 3.25 | 0.01 |
| **Settlement** | 81.90 | 147.62 | 65.73 | 0.09 | 0.16 | 0.07 |
| **Bare surface** | 73.53 | 90.55 | 17.02 | 0.08 | 0.10 | 0.02 |
| **Woodland** | 186.64 | 187.02 | 0.38 | 0.20 | 0.20 | 0.00 |
| **TOTAL** | **94,026.51** | **94,026.51** | | **100** | **100** | |

### 3.3 Transition Potential Modeling based on Artificial Neural Network (ANN)

Transition potential analysis provides the level of performance of the ANN algorithm to generate simulated land cover data. Figure 2 shows the neural network learning curve with the red and green curves depicting the behavior of the neural training and validation, respectively. The spike in the graph shows the largest error possible at the 1,000th training sample level, which was further corrected as the training progresses thus eliminating both issues of unrepresentative train dataset and unrepresentative validation dataset. The representative test of good fit of the neural training is presented in Table 4. It shows that training of dataset returned 69.019% and 68.165% level of accuracy for the years 2015 and 2050, respectively. Meanwhile, the validation accuracy was found as 76.203% and 75.877% for the years 2015 and 2050, respectively.

**Table 4.** ANN training validation analysis

| Parameters | 2015 simulation value | 2050 simulation value |
|---|---|---|
| Scale for training | 80% | 80% |
| Scale for validation | 20% | 20% |
| Hidden neurons | 10 | 10 |
| Learning rate | 0.05 | 0.05 |
| iterations | 5,000 | 5,000 |
| Training of dataset | 69.019% | 68.165% |
| Accuracy of validation dataset | 76.203% | 75.877% |

Transition potential describes the foundation and conversion pathway with probability matrix which shows the transfer direction of land cover classes from a particular period to another. For this study, Table 5 describes the Markovian transition probability matrix for the eight land cover classes for the period 2002-2012. Overall, settlement (1.000), woodland (0.9995), waterbody (0.9987) and cropland (0.9965) had the highest Markovian probabilities while shrubland (0.7957) had the least indicating the range of possibilities to remain unchanged in the future. In terms of transformation to other land cover classes, cropland had the highest Markovian probabilities, thus, it can transform to cropland, shrubland, grassland, settlement, bare surface and woodland with values of 0.9965, 0.1705, 0.0293, 0.0012 and 0.0005, respectively. Woodland was found to have the least dynamic probability to change to other land cover classes apart from self-transformation. This makes woodland less likely to change overtime.

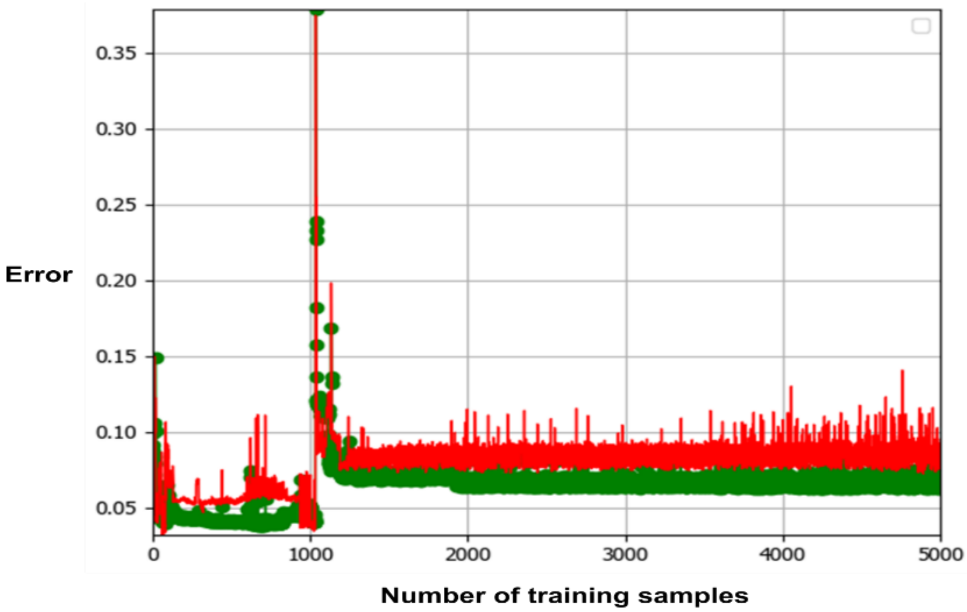


**Figure 2.** Neural network learning curve for the study with 5,000 training samples. The green curve shows the neural train generated from the training sample and the red curve shows the associated neural train validation

**Table 5.** Markovian transition probability matrix of land cover classes from 2002 to 2012

| Land cover | Cropland | Agroforestry | Shrubland | Grassland | Waterbody | Settlement | Bare surface | Woodland |
|---|---|---|---|---|---|---|---|---|
| **Cropland** | 0.9965 | 0.0000 | 0.0012 | 0.0017 | 0.0000 | 0.0006 | 0.0000 | 0.0000 |
| **Agroforestry** | 0.0000 | 0.9840 | 0.0106 | 0.0036 | 0.0000 | 0.0018 | 0.0000 | 0.0000 |
| **Shrubland** | 0.1705 | 0.0331 | 0.7957 | 0.0000 | 0.0007 | 0.0000 | 0.0000 | 0.0000 |
| **Grassland** | 0.0293 | 0.011 | 0.0024 | 0.953 | 0.0018 | 0.0004 | 0.0021 | 0.0000 |
| **Waterbody** | 0.0000 | 0.0000 | 0.0003 | 0.0005 | 0.9987 | 0.0005 | 0.0000 | 0.0000 |
| **Settlement** | 0.0000 | 0.0000 | 0.0000 | 0.0000 | 0.0000 | 1.0000 | 0.0000 | 0.0000 |
| **Bare surface** | 0.0012 | 0.0000 | 0.0000 | 0.0098 | 0.0025 | 0.0000 | 0.9865 | 0.0000 |
| **Woodland** | 0.0005 | 0.0000 | 0.0000 | 0.0000 | 0.0000 | 0.0000 | 0.0000 | 0.9995 |

### 3.4 Cellular Automata (CA) based Dynamics of Land Cover Simulation

The result of the Markovian transitions stated in Table 5 generates three types of land cover results as determined by CA. The first is transition potential maps, which spatially display the probabilistic potential of one land cover class to change to another with values ranging from 0 to 100 indicating levels of land cover transition. A total of 41 maps were generated with cropland having strongest connection to all other 7 land cover classes. Second is the certainty raster, which is the difference between large transition potential maps of the two periods 2002 and 2012. The largeness of the transition potential maps creates room for the degree of occurrence of the land cover classes in the predicted and simulated land cover classes.

Thus, Figure 3 depicts the certainty raster for the years simulated 2015 and the predicted 2050. Transitional certainty for the simulated year 2015 depicts some varying ranges while that of the predicted 2050 returned proportions that is quasi-equal showing the pattern of anticipated land cover changes for the two periods.

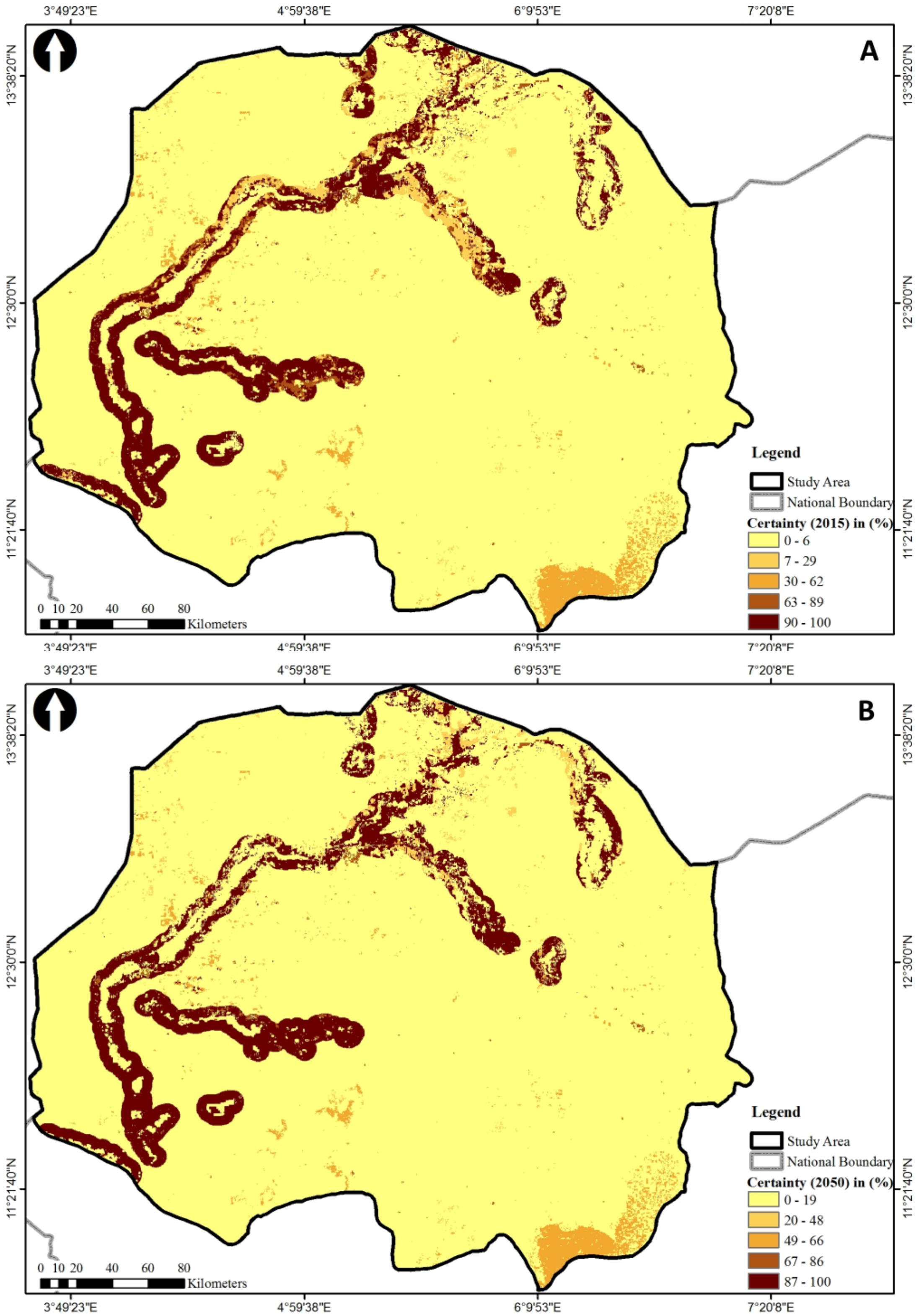


**Figure 3.** Certainty raster showing the spatial differentials in transition potentials for 2015 (a) and 2050 (b)

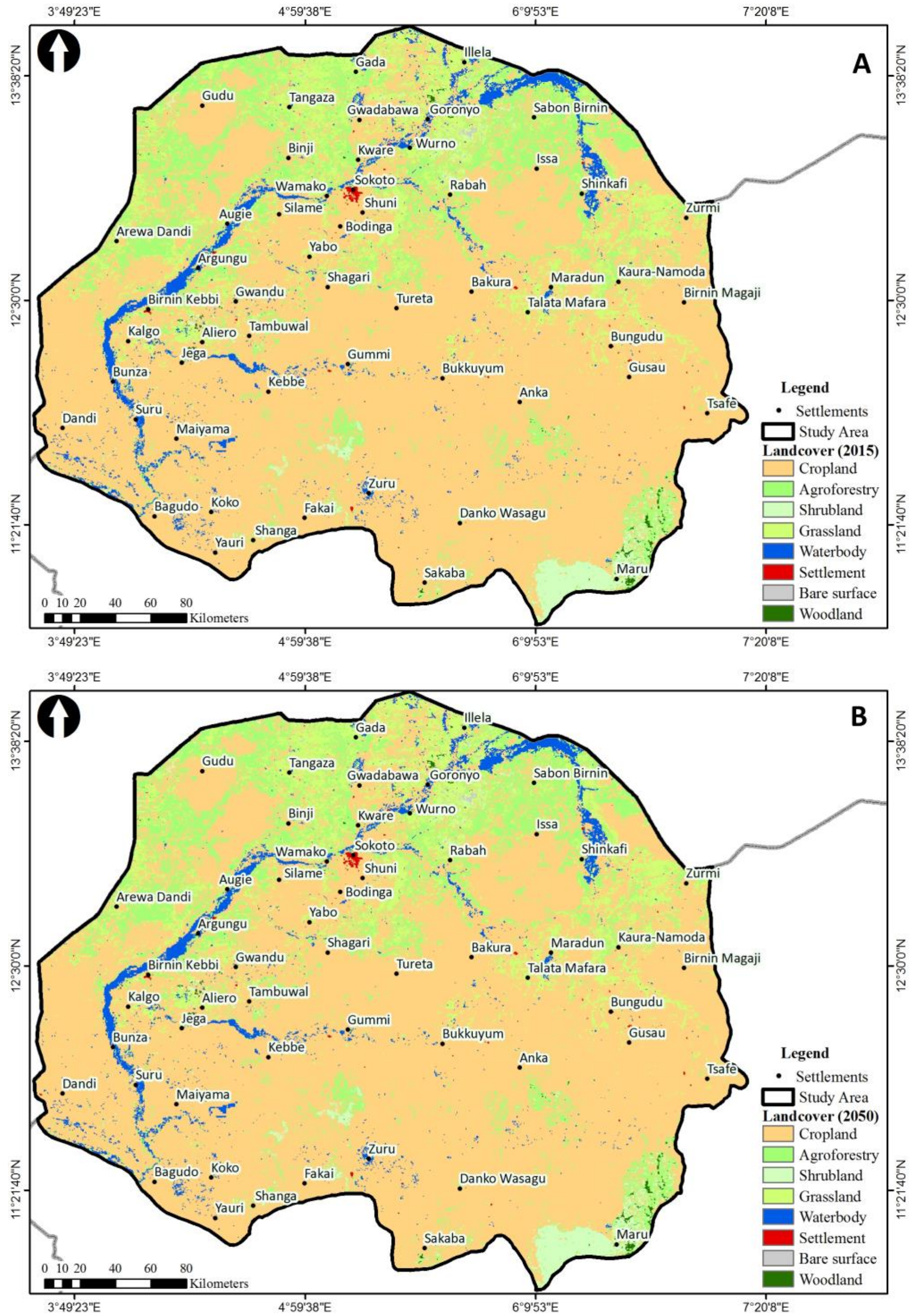


**Figure 4.** Simulated land cover for the years 2015 (a) and 2050 (b)

The third output is the 2015 simulated land cover and the predicted 2050 land cover (Figure 4). The corresponding land area and proportion for the simulated and predicted land cover datasets are specified in Table 7. In terms of proportionality, there exists some quasi-symmetric similarities. Cropland dominated the area with 73.02% (68,829.272 $km^2$) as simulated for 2015 and by 2050 as predicted, it will decrease to 73.126% (68,758.191 $km^2$) while woodland occupied the least proportion and land area with 0.198% (185.945 $km^2$) simulated for 2015 and as predicted for 2050, it will occupy 0.197% (185.315 $km^2$) of the Sokoto-Rima basin.

In terms of predicted changes, by 2050, it is expected that reductions will be observed in cropland, agroforestry, waterbody, bare surface and woodland while grassland and settlement will expand spatiotemporally.

**Table 6.** Proportion of the simulated land cover (2015) and predicted land cover (2050)

| Land cover class | Simulated 2015 land area (km$^2$) | Proportion (%) | Predicted 2050 land area (km$^2$) | Proportion (%) | Land Change (km$^2$) | Change (%) |
|---|---|---|---|---|---|---|
| **Cropland** | 68,829.272 | 73.202 | 68,758.191 | 73.126 | -71.081 | -0.076 |
| **Agroforestry** | 11,705.373 | 12.449 | 11,653.121 | 12.393 | -52.252 | -0.056 |
| **Shrubland** | 1,690.986 | 1.798 | 1,690.536 | 1.798 | -0.45 | 0 |
| **Grassland** | 8,324.121 | 8.853 | 8,451.328 | 8.988 | 127.207 | 0.135 |
| **Waterbody** | 3,053.235 | 3.247 | 3,050.172 | 3.244 | -3.063 | -0.003 |
| **Settlement** | 147.837 | 0.157 | 148.288 | 0.158 | 0.451 | 0.001 |
| **Bare surface** | 89.729 | 0.095 | 89.549 | 0.095 | -0.18 | 0 |
| **Woodland** | 185.945 | 0.198 | 185.315 | 0.197 | -0.63 | -0.001 |
| **TOTAL** | **94,026.50** | **100** | **94,026.50** | **100** | | |

### 3.5 Validation of Land Cover Simulation

Table 7 showed the model performance of both simulated 2015 land cover and predicted 2050 datasets. The statistics for kappa location, histogram and overall showed closeness to 1, which indicates a strong agreement. Importantly, the overall percentage of correctness showed that the 2015 simulated land cover dataset returned 88.01%, while the 2050 predicted land cover data returned 87.87%, showing strong performance of the simulation and prediction tasks (Geri et al. 2011). The 2050 dataset is therefore suitable to be used to model future ecosystem services.

**Table 7.** Kappa index of the model validation for the simulated and predicted land cover datasets

| Model validation parameter | Simulated 2015 | Predicted 2050 |
|---|---|---|
| Kappa (location) | 0.9378 | 0.9279 |
| Kappa (histogram) | 0.9606 | 0.9674 |
| Kappa (overall) | 0.9142 | 0.9116 |
| % of correctness | 88.0124 | 87.8714 |

### 3.6 Nature of Baseline Ecosystem Services

*Crop Production (2015);* Five levels of crop production indicated by crop yields were detected: very low (0-0.58 tonnes/km$^2$), low (0.58-1.59 tonnes/km$^2$), moderate (1.59-2.63 tonnes/km$^2$), high (2.63-3.87 tonnes/km$^2$) and very high (3.87-6.16 tonnes/km$^2$) (Table 8). The aggregate of low and very low yield statuses constitute 56.64% while moderate status comprises 21.88%, showing that the crop yield scale in the Sokoto-Rima basin is average. This productivity level affirmed the assertion that crop production in the area is small-scale, which is producing at low level while areas with high crop yield status occupy roughly 21% of the land area. Spatially, these productivity levels can be observed in Figure 5, indicating low productivity are scattered throughout the study area while high yields can be identified in some location at the western, eastern and southern axis of the Sokoto-Rima basin.

**Table 8.** Areal extent of aggregate crop yields status for the static year 2015

| Status of aggregate crop yield (tonnes/km$^2$) | Land area (km$^2$) | Proportion (%) |
|---|---|---|
| **Very low (0-0.57)** | 27,751.64 | 30.42 |
| **Low (0.57-1.59)** | 24,742.45 | 26.22 |
| **Moderate (1.59-2.63)** | 20,749.85 | 21.88 |
| **High (2.63-3.87)** | 13,943.02 | 14.51 |
| **Very high (3.87-6.16)** | 6,839.53 | 6.97 |
| **Total** | **94,026.50** | **100.00** |

*Seasonal Water Yield (2015);* Hydrological processes of quick flow define the nature of water provision in a particular basin as defined by the SWY model. As shown in Table 9, seasonal water ranges from very low (0-88.69 mm) to very high (813.24-1155 mm) in the Sokoto-Rima basin. As expected of a typical dryland, 61% of the area has low SWY status while 23.18% fall under areas with high SWY and 15.83% moderate SWY. The lower section of Figure 5 shows the hydrological network of streams and rivers feeding main water bodies (Sokoto and Rıma Rivers) which defines the level of seasonal water in the basin. However, there exists a clearly marked spatial delineation between the north and the south in the former is characterized by low SWY and the latter high SWY.

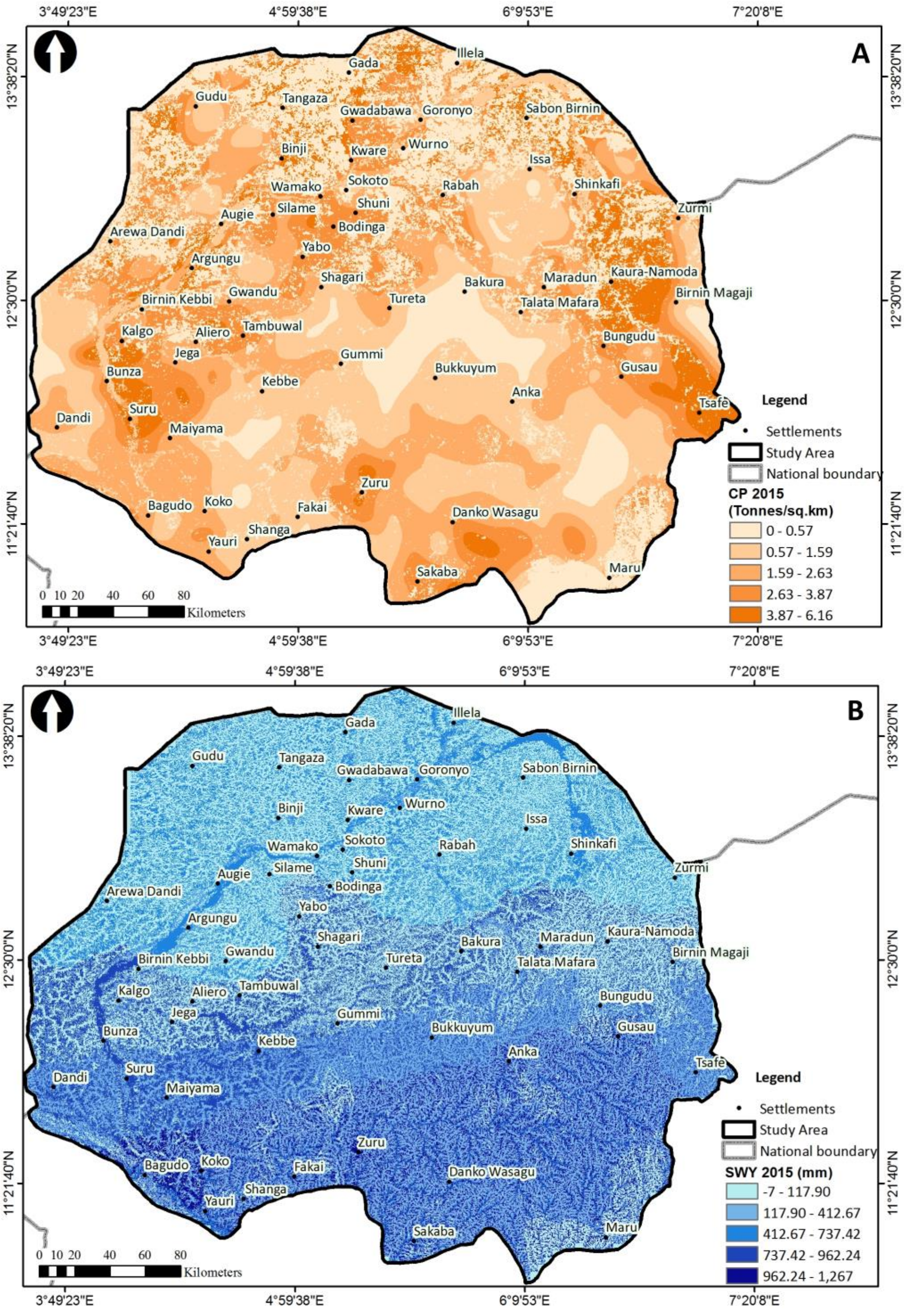


**Figure 5.** Spatial distribution of crop production (a) and seasonal water yield (b) for the Sokoto-Rima basin in 2015

**Table 9**: Proportion of SWY status in the study area for the static year 2015

| Status/modelled SWY (mm) | Land area (km$^2$) | Proportion (%) |
|---|---|---|
| **Very low (0-88.69)** | 34,127.55 | 36.30 |
| **Low (88.69-320.21)** | 23,220.20 | 24.70 |
| **Moderate (320.21-599.06)** | 14,889.05 | 15.83 |
| **High (599.06-813.24)** | 13,472.80 | 14.33 |
| **Very high (813.24-1155)** | 8,316.90 | 8.85 |
| **Total** | **94,026.5** | **100.00** |

*Habitat Quality (2015)*; HQ expresses ecosystem integrity in terms of its intactness and capacity to supply ecosystem services within a specific area coupled with ability to withstand degradation (Terrado et al. 2016). The 2015 HQ of the Sokoto-Rima basin showed that very high status comprises 3.25% (3,057.32 km$^2$), high status comprises 10.40% (9,778.23 km$^2$), moderate status comprises 12.97% (12,195.08 km$^2$) and very low status comprises 73.38% (68,995.87 km$^2$) (Table 10). This outcome is spatially expressed in Figure 6a, which is dominated by low HQ status. Also, high status was restricted to spots of protected vegetation particularly woodland, showing that level of biodiversity is very low and the possibility of degradation of natural habitats is very high in the study area. Although, the semi-arid ecosystem is often characterized by low grass and tree density, issues of high land clearance for cultivation in the Sokoto-Rima basin has been prevalent for years (Olagunju, 2015), which is a pointer to high level of degradation in HQ detected. Furthermore, this was stated by Oladipo (1995) to be responsible for increasing instances of southward migration of the Sahara Desert which has hampered the level of biodiversity and quality of the protected areas of the northern part of Nigeria including the Sokoto-Rima basin.

**Table 10**: Proportion of HQ status in the study area for 2015

| Status/HQ level | Land Area (km$^2$) | Proportion (%) |
|---|---|---|
| **Very high (0.799-1.0)** | 3,057.32 | 3.25 |
| **High (0.342-0.799)** | 9,778.23 | 10.40 |
| **Moderate (0.175-0.342)** | 12,195.08 | 12.97 |
| **Very low (0-0.124)** | 68,995.87 | 73.38 |
| **Total** | **94,026.50** | **100.00** |

*Nutrient retention ratio (2015)*; NRR directly measures the extent of nutrient cycling in space and it is a vital approach in explaining the spatial flow of nutrient within a given ecosystem. The nature of NRR as shown in Table 11 states that very high constitutes 6,196.88 km$^2$ (6.59%), high constitutes 6,104.74 km$^2$ (6.49%), moderate constitutes 12,744.18 km$^2$ (13.55%), low constitutes 24,777.04 km$^2$ (26.35%) and very low constitutes 44,203.66 km$^2$ (47.01%) of the Sokoto-Rima basin. The low distribution of NRR over space as shown in Figure 6 showed that the quick uptake of nutrient is directly proportional to the dominant typology of land cover in the study area. Spatially nutrients retention observed at edges of river systems showed high potentials while those at the cultivated areas such as wetlands and crop cultivation complexes showed moderate to low statuses thus establishing the classification posited by Salata et al. (2017).

**Table 11**: Proportion of NRR status in the study area for 2015

| NRR Level | Land Area (km$^2$) | Proportion (%) |
|---|---|---|
| **Very high (0.8-1.0)** | 6,196.88 | 6.59 |
| **High (0.6-0.8)** | 6,104.74 | 6.49 |
| **Moderate (0.4-0.6)** | 12,744.18 | 13.55 |
| **Low (0.2-0.4)** | 24,777.04 | 26.35 |
| **Very low (0-0.2)** | 44,203.66 | 47.01 |
| **Total** | **94,026.50** | **100.00** |

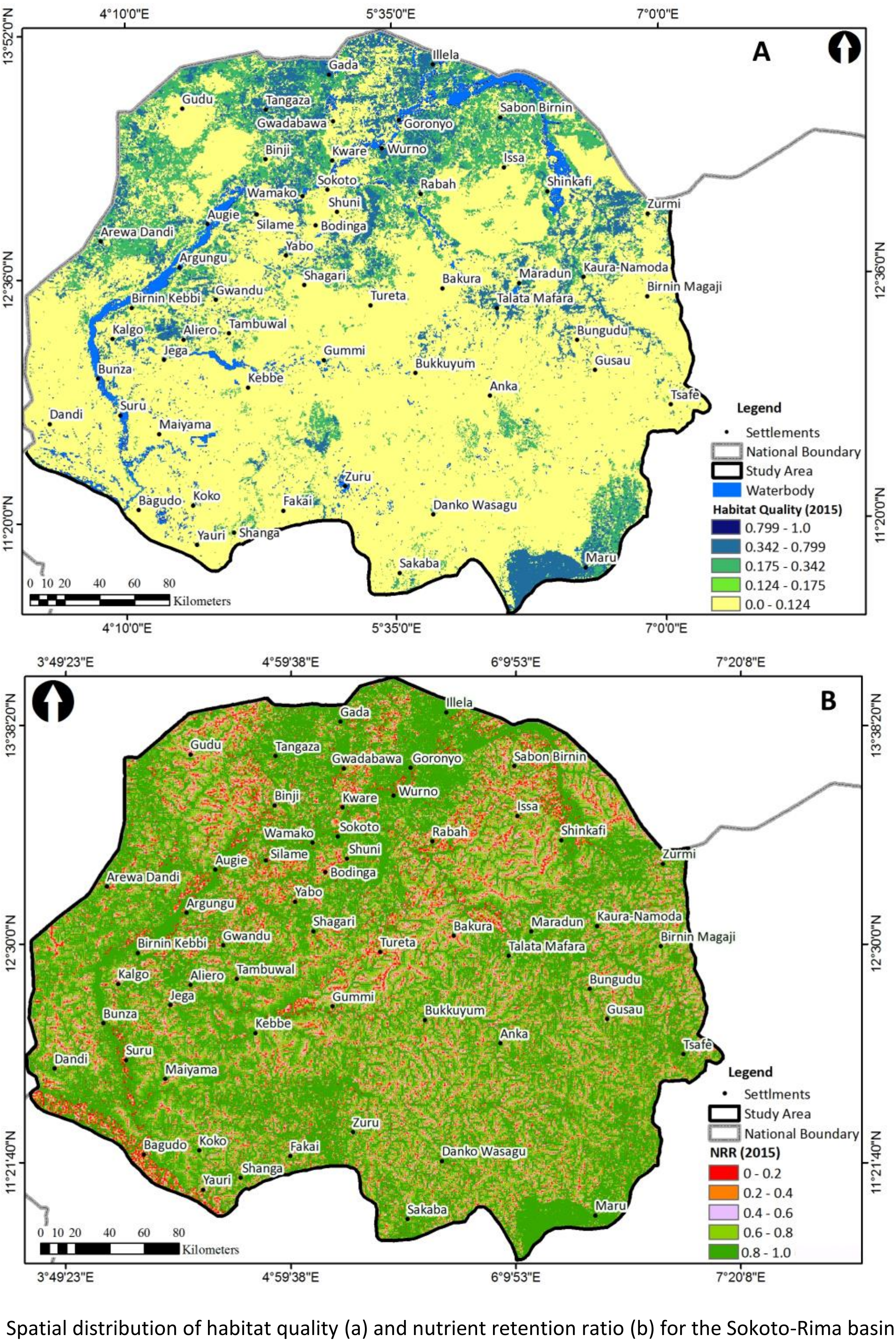


**Figure 6.** Spatial distribution of habitat quality (a) and nutrient retention ratio (b) for the Sokoto-Rima basin in 2015

## 3.7 Future Ecosystem Services (2050)

*Crop production (2050);* By 2050, CP status will remain unchanged, sustaining the average crop yield level with the prior observed five levels of crop yield. Very low status will occupy 23.49% (22,089.40 km$^2$), low status 32.99% (31,019.28 km$^2$), moderate 22.03% (20,713.01 km$^2$), high 14.59% (13,715.10 km$^2$) and very high status 6.9% (6,489.71 km$^2$) in the study area. In comparison with the 2015 crop production, crop yield in terms of tonnage per land area will remain averagely low, signifying no systematic change in productivity levels in the Sokoto-Rima basin.

Spatially, Figure 7a shows that CP status in 2050 will show some localized differences compared with 2015 with improvements in the degree of low status in areas such as Anka, Bukkuyum and Shanga in the central, and southern zones of the study area.

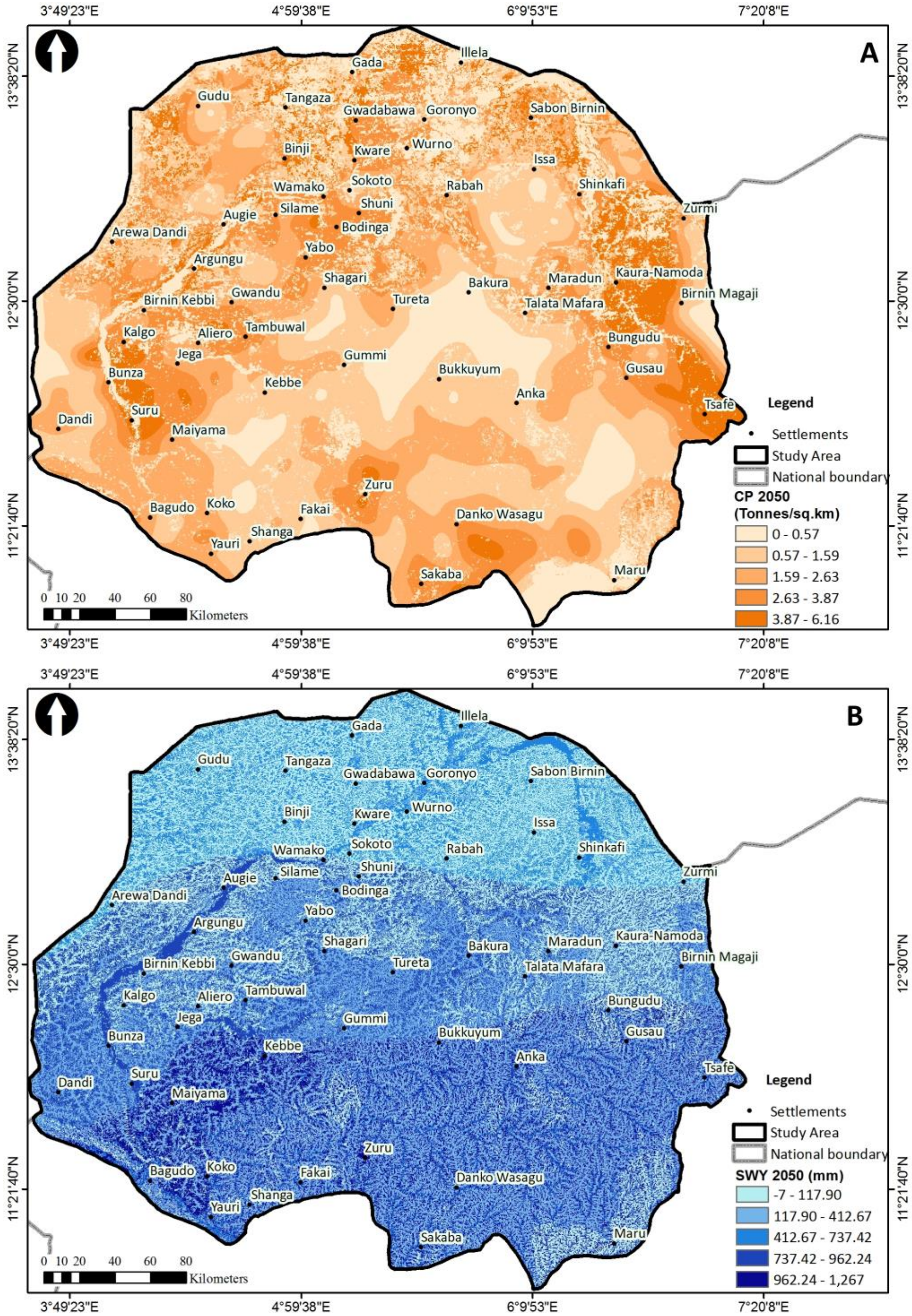


**Figure 7.** Spatial distribution of simulated crop production (a) and seasonal water yield (b) for the year 2050

*Seasonal water yield (2050)*; The status levels observed in 2015 will be maintained by 2050 with some differences in land area and proportions. As shown in Figure 7, Very low yield will occupy 28.42% (26,718.17 km$^2$), low 31.61% (29,721.67 km$^2$), moderate 11.96% (11,243.45 km$^2$), high 14.43% (13,570.08 km$^2$) and very high statuses will occupy, 13.58% (12,773.13 km$^2$) of the landscape correspondingly.

Natural water flow from hydrological sources specifically quick flow (runoff) from rainfall will slightly improve the seasonally available water in the Sokoto-Rima basin. This could be stimulated variations in climatic parameters of the study area. As shown in Figure 7b, improvements will be observed in low, high and very statuses in close to the major rivers, the water reservoirs, and the hilly areas of the eastern axis of the study area. Areas such as Suru, Maiyama, Kebbe, Bunza, Bagudo and Yauri in the southern axis are expected to experience high SWY by 2050.

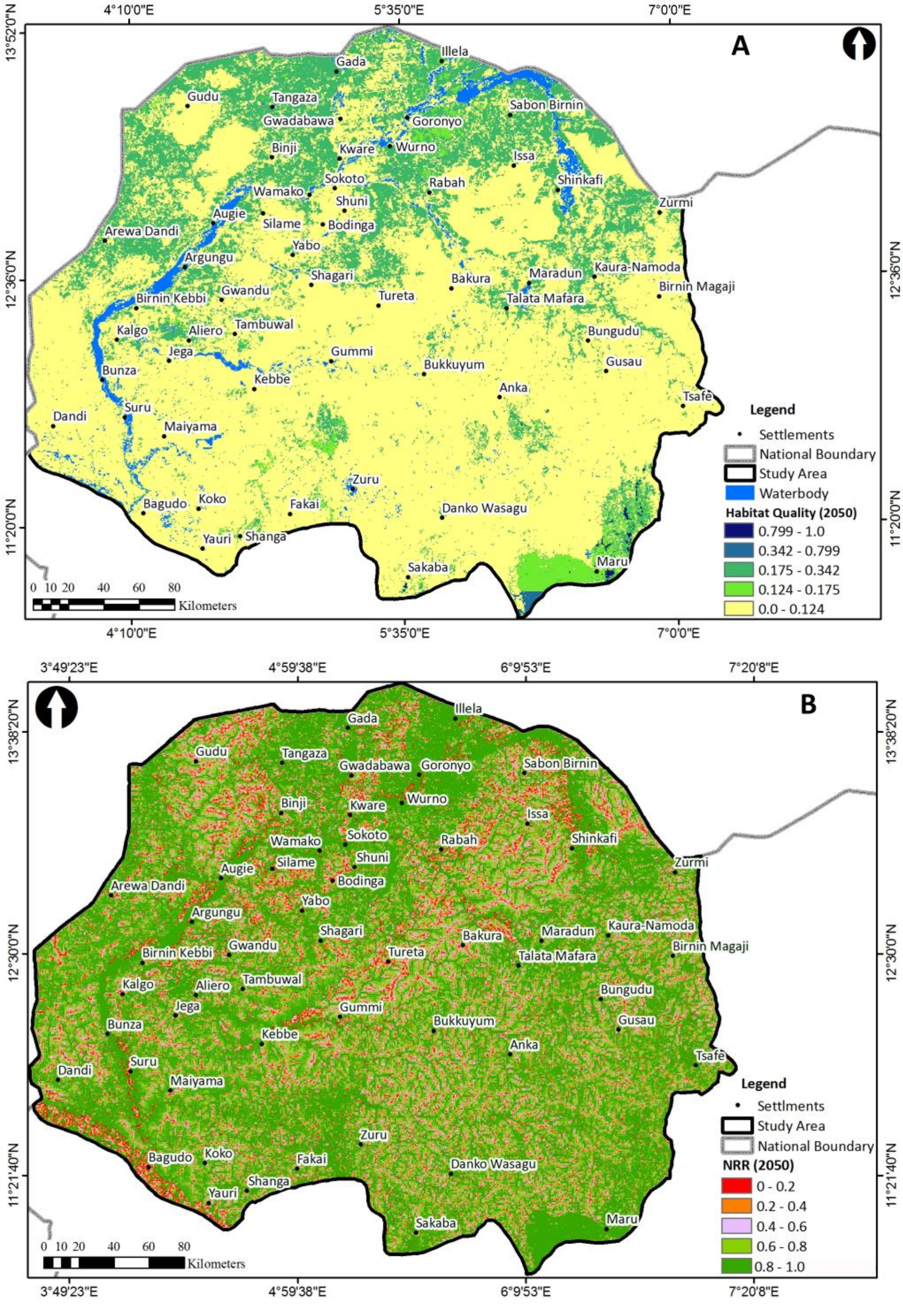


**Figure 8.** Spatial distribution of simulated habitat quality (a) and nutrient retention ratio (b) for the year 2050

*Habitat quality (2050)*; Slight improvements in habitat quality will surface in 2050 as the HQ levels will increase to five from the four levels observed in 2015. Very high HQ status will occupy 0.12% (114.61 km2), high HQ 0.25% (231.48 km2), moderate HQ 21% (19,741.73 km$^2$), low HQ 2.15% (2,018.09 km$^2$) and very low HQ 76.49% (71,920.59 km$^2$) of the landscape. This shows that some of the high levels will be lost to lower HQ status, an observation of reduction in biodiversity. Figure 8a testifies spatially to this assertion with high biodiversity areas projected in localized communities such as northern areas of Zuru and areas surrounding Maru at the southeastern axis of the Sokoto-Rima basin.

*Nutrient retention ratio (2050)*; Retention of nutrient will be proportionally similar but slightly different in terms of land area, thus sustaining the agrarian cum semi-arid ecosystem pattern. As shown in Figure 8b, very low NRR will amount to 6.58% (6,190.64 km$^2$) of the landscape, low NRR will constitute 6.51% (6,125.49 km$^2$), moderate will occupy 13.76% (12,935.24 km$^2$), high will constitute 26.8% (25,200.32 km$^2$) and very high 46.34% (43,574.8 km$^2$) of the study area. Compared to 2015 status, a meagre change is anticipated by the year 2050. This could be related to the linkage of nutrient retention to the natural land surface configuration such as soil characteristics and terrain features which usually remain largely unchanged. However, 1.7% increase in high status could be related to possibility of more water within the basin as depicted as affirmed by the 2050 SWY represents an improvement in available nutrient flow within the Sokoto-Rima basin by the year 2050.

## 4. Conclusion

Quantifying the status and dynamic patterns of ecosystem services is dependent on spatially explicit models which are inherently reliant on land cover and its associated spatial data. A key aspect of this is predicting future land cover in order to produce future ecosystem services. To simulate and predict future land cover of any location, key spatial drivers spanning natural and anthropogenic activities are essential. In this study, an attempt was made to predict and simulate future land cover of the Sokoto-Rima basin of north-western Nigeria. These predicted and simulated datasets were used as principal data for the simulation of future ecosystem services using ecosystem service models embedded in InVEST software. The result showed that proximate and underlying drivers are important in future land cover prediction. Also, provisioning and regulating ecosystem services drive the functioning of the semi-arid ecosystem of the Sokoto-Rima basin. Correlation analysis of the geo-environmental variables showed that multi-collinearity effects have been eliminated from the data and CA-ANN is a suitable land cover prediction method for simulating future land cover of the study area. Crop production has shown that the Sokoto-Rima basin is indeed a low-producing agrarian ecosystem with average tonnage of crop produced in 2015 and similar pattern will be replicated by 2050. Seasonal water yields are highly variable, fluctuating between low to moderate water quantity required for proper functioning which is a typical trait of a dryland such as the semi-arid Sokoto-Rima basin. Habitat quality however showed that biodiversity will reduce as the years go by, requiring measures to resuscitate the dwindling natural ecological resources of the basin. The crop production model of InVEST provides a coarse global crop output within an area of less heterogeneous landscape and land management. Land management based crop fertilization rates provided by Tarfa et al. (2017) has provided a gap filling merit to address this drawback however engagement of localized crop yields and influence of land tenure systems can be assessed under a climate change scenario to check this drawback. In addition, the quick flow approach adopted from the InVEST's seasonal water yield model is based on surface water which is a determinant factor for sustenance of life for the dryland region. Basin scale hydrology is required to fully capture the pattern of water resource of the Sokoto-Rima basin.

Anthropogenic influence on the Sokoto-Rima basin will increase in the future and the persistence of this trend require checks and balances that will enshrine proper land use policy and sustainable environmental development. Woodland development through the Great Green Wall program can be up-scaled to the level of communities in a synergistic fashion with crop production (Davies, 2017). When adopted, this approach will also revive the dwindling level of the existing protected areas. This will secure existing agrarian system, improve ecological integrity, ensure regulated water availability, and nutrient flow within the natural and anthropogenic ecosystems will improve overtime. Moreover, ecosystem service interaction and integration to biodiversity management within the Sokoto-Rima basin can be pursued both at the watershed and local government levels in the study area.

## Acknowledgements

The authors appreciate the kind permission of the following organizations for the granting data access; European Space Agency (ESA) for the land cover data, Japanese Aerospace Exploration Agency (JAXA) for the datasets on terrain, Princeton Climate Analytics (PCA) for the climate data, United States Geological Survey (USGS) for soil, NDVI and evapotranspiration datasets and National Bureau of Statistics of Nigeria (NBS) for the population data. Finally, we greatly acknowledge the efforts of the three anonymous reviewers in improving the quality of paper.

## References


Davies, J. (2017). Biodiversity and the great green wall: Managing nature for sustainable development in the sahel. Ouagadougou: IUCN, xiv + 66 pp.

Defourny, P., Bontemps, S., Martin, B., Brockman, C., Fomferra, N., Grit, K., & Krüger, O. (2011). Landcover CCI: Product Specification Document. Year 2 Version 1.3.

Fasona, M. J., Soneye, A. S., Ogunkunle, O. J., Adeaga, O. A., Fashae, O. A., & Abbas, I. I. (2014). Simulating Land-Cover and Land-Use Change in the Savanna Under Present Day and Future Climate Scenarios-A GIS-Based Approach. *Earth Science Research*, *3*(1), 25.

Fasona, M., Omojola, A., Adeaga, O., & Dabi, D. (2007). Aspects of Climate Change and Resource Conflicts in the Nigeria Savannah. In *Report of IPCC/TGICA Expert Meeting on Integrating Analysis of Regional Climate Change and Response Options* (pp. 45-55).

Fu, Q., Li, B., Hou, Y., Bi, X., & Zhang, X. (2017). Effects of land use and climate change on ecosystem services in Central Asia's arid regions: a case study in Altay Prefecture, China. *Science of the Total Environment*, *607*, 633-646.

Geri, F., Amici, V., & Rocchini, D. (2011). Spatially-based accuracy assessment of forestation prediction in a complex Mediterranean landscape. *Applied Geography*, *31*(3), 881-890.

Haines-Young R., & Potschin M. (2018). *Common International Classification of Ecosystem Services* (CICES) V5.1.

Hølleland, H., Skrede, J., & Holmgaard, S. B. (2017). Cultural heritage and ecosystem services: A literature review. *Conservation and ManageMent of arChaeologiCal sites*, *19*(3), 210-237.

Huber, R., Rigling, A., Bebi, P., Brand, F. S., Briner, S., Buttler, A., ... & Lischke, H. (2013). Sustainable land use in mountain regions under global change: synthesis across scales and disciplines. *Ecology and Society*, *18*(3), 36, doi:10.5751/es-05499-180336.

Lambin, E. F., Geist, H. J., & Lepers, E. (2003). Dynamics of land-use and land-cover change in tropical regions. *Annual review of environment and resources*, *28*(1), 205-241.

MEA. (2005a). Ecosystem and Human Well-Being: Synthesis. Millennium Ecosystem Assessment, Island Press, Washington, DC.

MEA. (2005b). Ecosystem and Human Well-Being: Biodiversity Synthesis. Millennium Ecosystem Assessment, World Resources Institute, Washington, DC.

Mueller, N. D., Gerber, J. S., Johnston, M., Ray, D. K., Ramankutty, N., & Foley, J. A. (2012). Closing yield gaps through nutrient and water management. *Nature*, *490*(7419), 254-257.

Oguntunde, P. G., Abiodun, B. J., & Lischeid, G. (2011). Rainfall trends in Nigeria, 1901–2000. *Journal of Hydrology*, *411*(3-4), 207-218.

Oladipo, E. O. (1995). Some statistical characteristics of drought area variations in the savanna region of Nigeria. *Theoretical and Applied climatology*, *50*(3-4), 147-155.

Olagunju, T. E. (2015). Drought, desertification and the Nigerian environment: A review. *Journal of Ecology and the Natural Environment*, *7*(7), 196-209.

Oyebande, L., & Odunuga, S. (2010). Climate change impact on water resources at the transboundary level in West Africa: the cases of the Senegal, Niger and Volta Basins. *The Open Hydrology Journal*, *4*(1), 163-172.

Pérez-Hoyos, A., Rembold, F., Kerdiles, H., & Gallego, J. (2017). Comparison of global land cover datasets for cropland monitoring. *Remote Sensing*, *9*(11), 1118, doi:10.3390/rs9111118.

Roche, P. K., & Campagne, C. S. (2017). From ecosystem integrity to ecosystem condition: a continuity of concepts supporting different aspects of ecosystem sustainability. *Current opinion in environmental sustainability*, *29*, 63-68.

Salata, S., Garnero, G., Barbieri, C. A., & Giaimo, C. (2017). The integration of ecosystem services in planning: An evaluation of the nutrient retention model using InVEST software. *Land*, *6*(3), 48, doi:10.3390/land6030048.

Satya, B. A., Shashi, M., & Deva, P. (2020). Future land use land cover scenario simulation using open source GIS for the city of Warangal, Telangana, India. *Applied Geomatics*, 1-10.

Setten, G., Stenseke, M., & Moen, J. (2012). Ecosystem services and landscape management: three challenges and one plea. *International Journal of Biodiversity Science, Ecosystem Services & Management*, *8*(4), 305-312.

Sharp, R., Tallis, H. T., Ricketts, T., Guerry, A. D., Wood, S. A., Chaplin-Kramer, R., Nelson, E., Ennaanay, D., … & Douglass, J. (2018). InVEST 3.5.0. User’s Guide. The Natural Capital Project, Stanford University. University of Minnesota, The Nature Conservancy, and World Wildlife Fund.

Tarfa, B. D., Amapu, I. Y., Daudu, C. K., Arunah, U. L., Shero, I. A., Isah, A. S., Yakubu, A. A., Abdu, N., … & Ugbabe, O. O. (2017). Optimizing fertilizer use within the context of integrated soil fertility management in Nigeria. In C. S. Wortmann, & K. Sones (eds.), Fertilizer Use Optimization in Sub-Saharan Africa (pp. 148–163). Nairobi: CAB International.

Terrado, M., Sabater, S., Chaplin-Kramer, B., Mandle, L., Ziv, G., & Acuña, V. (2016). Model development for the assessment of terrestrial and aquatic habitat quality in conservation planning. *Science of the total environment*, *540*(1), 63-70.

Wangai, P. W., Burkhard, B., & Müller, F. (2016). A review of studies on ecosystem services in Africa. *International journal of sustainable built environment*, *5*(2), 225-245.

Yang, S., Zhao, W., Liu, Y., Wang, S., Wang, J., & Zhai, R. (2018). Influence of land use change on the ecosystem service trade-offs in the ecological restoration area: Dynamics and scenarios in the Yanhe watershed, China. *Science of the total environment*, *644*, 556-566.